Numerical tests of a generalized multilevel vibronic coupling formalism

Y. Won, R. Lagos, and R. Friesner
Department of Chemistry, University of Texas at Austin, Austin, Texas 78712

(Received 21 October 1985; accepted 19 February 1986)

An approximate matrix continued fraction method for calculating optical line shapes of molecular systems with multilevel excited state manifolds is compared with converged basis set results. It is shown that the theory gives correct spectral envelopes for all parameter values studied.

I. INTRODUCTION

The coupling of Born–Oppenhemier surfaces by vibrational degrees of freedom (and the consequent breakdown of the Born–Oppenheimer approximation) is an important effect in many processes in chemical physics. For systems with well-defined minimum configurations, an expansion of the coupling in powers of the vibrational coordinates is often rapidly convergent. This type of approximation is presently necessary if explicit solutions are desired for complicated systems.

The simplest models include only a linear dependence of the Hamiltonian on the vibrational coordinate. Such models have been widely utilized in studying a variety of spectroscopic and dynamical problems, e.g., spectroscopy of mixed valence compounds,[13,14] Jahn–Teller systems,[17] radiationless transitions,[18,19] electron transfer,[20] and absorption and circular dichroism of molecular aggregates.[4–9]

The most elementary linear vibronic coupling Hamiltonian consists of two electronic states coupled to a single vibrational mode. This problem, which can be accurately solved numerically,[10,11] has been studied by a number of workers using approximate techniques in order to obtain insight into the effects of vibronic coupling on the manifold of eigenstates.[4,12,15] From these investigations, the dependence of the energies and wave functions of the Hamiltonian parameters can be understood, and several regions of parameter space can be delineated.

Reliable results from matrix diagonalization are limited to relatively small systems because basis set size grows rapidly as the number of electronic states and/or vibrational modes increases. For many realistic systems, therefore, one must resort to approximate methods.[2,3,7,8] The standard approach has been to use perturbation theory in either the electronic or vibronic coupling parameters. While this is often acceptable, there are substantial regions of parameter space for which no perturbative approach is accurate.[4] Thus, it would be desirable to have an efficient approximation technique which can be used for all coupling strengths in multilevel, multimode systems.

In a previous paper, we proposed such a method, based on a continued fraction algorithm suggested by Sumi[16] and generalized by us (via a matrix formulation) to explicitly incorporate molecular cluster interactions.[1,21] The present applications are to one-exciton optical properties of molecular systems with vibronic interactions among excited state levels (e.g., absorption, circular dichroism, linear dichroism); a treatment of molecular crystals is presented in Refs. 21 and 22.

In this paper, we report numerical results (compared with large basis set calculations) for a simplified version of the matrix continued fraction algorithm proposed in Ref. 1. We show that this approximation produces quantitative agreement for the spectral envelope with basis set results over a wide range of parameter values for two- and three-level excited electronic manifolds. The method is straightforward to implement numerically, computationally fast, and easily generalized, e.g., to continuous phonon bands. While only zero temperature results are presented here, preliminary work indicates that agreement and computational efficiency are comparable for a finite temperature version of the theory. As long as one does not require very high resolution spectra (e.g., for comparison with gas phase experiments), the present approach appears to have no obvious deficiency. Applications to experimental systems and extensions to two-particle properties (e.g., resonance Raman, density matrix evolution) are currently in progress.

II. THEORY

A. Effective Hamiltonian

Consider a coupled exciton–phonon system constructed with an electronic ground state, M interacting excited electronic levels, and N harmonic vibrational modes.

The ground state is taken to be a crude Born–Oppenheimer state with electronic energy E_g set equal to zero; the excited state surfaces are expressed in terms of the ground state normal coordinates, $\{Q_N\}_{n=1}^{N}$. In this paper only linear coupling terms in the excited-state potential energy surfaces are considered. The displacement of the normal coordinate of mode n, Q_n, in a state i corresponds to a diagonal term $\theta_{ii}^{(n)}$ in the vibronic coupling tensor $\boldsymbol{\theta}$. An exchange vibronic coupling of states i and j through mode n contributes an off-diagonal term with magnitude $\theta_{ij}^{(n)}$. The frequencies $\{\omega_n\}_{n=1}^{N}$ are taken to be independent of the electronic levels.

Taking the zero of energy to be

$$\frac{1}{N}\sum_{i=1}^{N}\epsilon_{ii} - E_g + \frac{1}{2}\sum_{i=1}^{N}\omega_n \quad (\hbar = 1),$$

the effective one-exciton excited state Hamiltonian is written in second quantized form as

$$H = \sum_{i,j=1}^{N}\epsilon_{ij}|i\rangle\langle j| + \sum_{n=1}^{M}\omega_n\, b_n^{\dagger}\, b_n + \sum_{n=1}^{M}\sum_{i,j}^{N}\theta_{ij}^{(n)}|i\rangle\langle j|(b_n + b_n^{\dagger}). \quad (1)$$

 0021-9606/86/126567-08$02.10

Here $|i\rangle$ is a projection operator for electronic level i with energy ϵ_{ii}, ϵ_{ij} is the off-diagonal electronic coupling between levels i and j, ω_n is the frequency of mode n, and $\theta_{ij}^{(n)}$ is a vibronic coupling parameter as explained above. $b_n^\dagger$ and b_n create and destroy a vibrational quantum in mode n, respectively. The normal coordinate Q_n can be expressed as

$$Q_n = \frac{1}{\sqrt{2}}(b_n + b_n^\dagger).$$

The singly excited states of the system are

$$\varphi_\alpha = \sum_{i,\mathbf{n}} C_{i\mathbf{n}}^{(\alpha)} |i,\mathbf{n}\rangle, \tag{2}$$

where

$$|i,\mathbf{n}\rangle = |i,n_1,n_2,...,n_M\rangle \tag{3}$$

denotes a crude Born–Oppenheimer basis state of electronic level $|i\rangle$ containing n_j vibrational quanta in mode j. In what follows we calculate optical transitions from the ground state vibronic levels to the one-exciton manifold spanned by this basis set.

B. Basis set method

The matrix elements for the Hamiltonian in Eq. (1) can easily be computed with the crude Born–Oppenheimer basis states [Eq. (3)]. The Hamiltonian matrix is then diagonalized numerically to give excited-state eigenvectors like Eq. (2) with excited-state energies E_α.

The ground state $|0,\mathbf{n}\rangle$ is a tensor product of noninteracting harmonic basis functions with n_j quanta in the jth mode.

$$|0,\mathbf{n}\rangle = |0\rangle|n_1\rangle|n_2\rangle...|n_N\rangle \tag{4}$$

for a general N mode system, where $|0\rangle$ is an exciton vacuum.

The electronic dipole moment operator $\boldsymbol{\mu}$ is defined as

$$\boldsymbol{\mu} = \sum_i \boldsymbol{\mu}_i [\,|0\rangle\langle i| + |i\rangle\langle 0|\,], \tag{5}$$

where $\boldsymbol{\mu}_i$ is the electronic transition dipole moment for the state i. The transition moment to the state α from the ground state is then

$$\langle 0,\mathbf{m}|\boldsymbol{\mu}|\varphi_\alpha\rangle = \sum_{i=1}^{N} \boldsymbol{\mu}_i C_{i\mathbf{m}}^{(\alpha)}. \tag{6}$$

For an isolated molecule, the optical absorption intensity $I(E)$ can be formulated as

$$I(E) = \frac{1}{Q}\sum_{\alpha,m} |\langle 0,\mathbf{m}|\mu|\varphi_\alpha\rangle|^2 \delta(E - E_\alpha) - \sum_n m_n\omega_n)\exp\Big(-\beta\sum_n m_n\omega_n\Big), \tag{7}$$

where $\beta = 1/kT$, and the partition function Q is

$$Q = \sum_m \exp\Big(-\beta\sum_n m_n\omega_n\Big). \tag{8}$$

$\delta(E)$ is the Dirac delta function. To take into account various line broadening effects, we replace $\delta(E)$ by the Lorentzian line shape function

$$L(E) = \frac{1}{\pi}\frac{\gamma}{E^2 + \gamma^2}, \tag{9}$$

where γ is a phenomenological damping factor. $I(E)$ is then evaluated by inserting the eigenvalues and eigenvectors obtained from the diagonalization procedure into Eqs. (6) and (7).

C. Matrix continued fraction method for one-exciton Green's function

Instead of explicitly computing eigenvalues and eigenvectors, it is possible to calculate the optical line shape directly from the one-exciton Green's function matrix. The Hamiltonian in Eq. (1) can be decomposed as $H = H_0 + V$ where

$$H_0 = \sum_{i,j=1}^{M} \epsilon_{ij}|i\rangle\langle j| + \sum_{n=1}^{N} \omega_n b_n^\dagger b_n \tag{10}$$

and

$$V = \sum_{i,j=1}^{M}\sum_{n=1}^{N} \theta_{ij}^{(n)}|i\rangle\langle j|(b_n + b_n^\dagger). \tag{11}$$

We first define matrices $\mathbf{G}(E)$, $\boldsymbol{\epsilon}$, and $\boldsymbol{\theta}_n$ whose elements are $G_{ij}(E)$, ϵ_{ij}, and $\theta_{ij}^{(n)}$, respectively. $\mathbf{G}(E)$ is the thermally averaged one-exciton Green's function matrix for Hamiltonian in Eq. (1):

$$\mathbf{G}(E) = \frac{1}{Q}\sum_{\mathbf{m}} \exp(-\beta\sum_n m_n\omega_n)\langle\mathbf{m}|\mathbf{D}(E)|\mathbf{m}\rangle, \tag{12}$$

where Q is the partition function, and $\mathbf{D}(E)$ is defined below. $\mathbf{G}_0(E)$ is the zeroth-order Green's function matrix associated with H_0 in Eq. (10) and can be easily calculated from

$$\mathbf{G}_0(E)^{-1} = (E - i\gamma)\mathbf{1} - \boldsymbol{\epsilon}, \tag{13}$$

where γ is the line broadening factor chosen the same as in Eq. (9).

For a single vibrational mode, $\langle m|\mathbf{D}(E)|m\rangle$ in Eq. (12) has a straightforward representation as a matrix continued fraction:

$$\langle m|\mathbf{D}(E)|m\rangle^{-1} = \mathbf{G}_0^{-1}(E) - \boldsymbol{\Gamma}_m^{(1)}(E) - \boldsymbol{\Gamma}_m^{(2)}(E), \tag{14}$$

where

$$\boldsymbol{\Gamma}_m^{(1)} = m\boldsymbol{\theta}\cfrac{1}{\mathbf{G}_0^{-1}(E+\omega) - (m-1)\boldsymbol{\theta}\cfrac{1}{\mathbf{G}_0^{-1}(E+2\omega) - (m-2)\boldsymbol{\theta}\cfrac{1}{\ddots}\boldsymbol{\theta}}\boldsymbol{\theta}}\boldsymbol{\theta} \tag{15}$$

and

$$\Gamma_m^{(2)} = (m+1)\boldsymbol{\theta}\frac{1}{\mathbf{G}_0^{-1}(E-\omega) - (m+2)\boldsymbol{\theta}\frac{1}{\mathbf{G}_0^{-1}(E-2\omega) - (m+3)\boldsymbol{\theta}\frac{1}{\cdots}\boldsymbol{\theta}}\boldsymbol{\theta}}\boldsymbol{\theta}. \tag{16}$$

At zero temperature only the $m = 0$ vibrational level is occupied and $\mathbf{G}(E)$ is reduced to $\langle 0|\mathbf{D}(E)|0\rangle$ with $\Gamma_0^{(1)} = 0$.

$$\mathbf{G}^{-1}(E) = \mathbf{G}_0^{-1}(E) - \Gamma_0^{(2)}(E). \tag{17}$$

For a general multimode system, no such expression exists; the exact continued fraction is highly branched and thus quite demanding computationally to evaluate. However, if the spectral envelope, rather than highly resolved vibrational lines, is of primary interest, a simple approximation to the multiply branched continued fraction gives quite good results.

For the multimode system at zero temperature,

$$\mathbf{G}^{-1}(E) = \mathbf{G}_0^{-1}(E) - \Gamma_0(E). \tag{18}$$

Our approximation consists of replacing the exact complicated branched structure for $\Gamma_0(E)$ with the expression

$$\Gamma_0(E) = \sum_n \boldsymbol{\theta}_n \frac{1}{G_0^{-1}(E-\omega_n) - 2\sum_n \boldsymbol{\theta}_n \frac{1}{G_0^{-1}(E-2\omega_n) - 3\sum_n \boldsymbol{\theta}_n \frac{1}{\cdots}\boldsymbol{\theta}_n}\boldsymbol{\theta}_n}\boldsymbol{\theta}_n. \tag{19}$$

This approximation has several attractive features. First, it is exact in two limits: the single mode (or narrow band) limit and through second order perturbation theory in the vibronic coupling tensor $\boldsymbol{\theta}$. Secondly, it is easy to implement numerically for an arbitrary (linearly coupled) exciton–phonon system, and is computationally efficient. Finally it is shown in Sec. III that, for line broadening of the order of the vibronic peak spacing, quantitatively accurate results are obtained when compared with basis set calculations for all parameter values studied. We also expect that, as the density of vibrational modes increases, the approximation becomes reliable without phenomenological broadening (because a Markov picture, in which sharp structures are washed out, becomes valid).

Having calculated $\mathbf{G}(E)$, the isotropic optical absorption intensity $I(E)$ is obtained from

$$I(E) = -\frac{1}{\pi}\sum_{i,j} \boldsymbol{\mu}_i \cdot \boldsymbol{\mu}_j \,\mathrm{Im}\, G_{ij}(E), \tag{20}$$

where $\boldsymbol{\mu}_i$ is defined in Eq. (5).

III. RESULTS

The optical absorption spectra for the two- and three-mode systems were calculated using both the approximate continued fraction and the basis set method as described in the previous sections. For comparison the spectra are normalized to make the area under the spectral line equal to 1.0.

We used a CDC Cyber 170/750 main frame for all calculations reported here. Because of the limitation of the allowed memory space in the computer, the basis set method implementation requires formulating the Hamiltonian matrix in a band storage mode. The employment of a banded matrix routine (e.g., EIGBS of the IMSL package) leads to considerable reduction in computational effort. Banded 450×450 matrices (225 vibrational basis functions for each electronic state) can easily be constructed and diagonalized to give eigenvalues and eigenvectors. A smaller Hamiltonian matrix, e.g., 162×162 (81 vibrational basis functions for each electronic state) was used for some small vibronic coupling tensors.

Without loss of generality, we take the electronic interaction matrix $\boldsymbol{\epsilon}$ to be diagonal:

$$\begin{bmatrix} J & 0 \\ 0 & -J \end{bmatrix} \text{ and } \begin{bmatrix} J & 0 & 0 \\ 0 & 0 & 0 \\ 0 & 0 & -J \end{bmatrix}$$

for two- and three-level systems, respectively. This situation can always be produced via canonical transformation of the electronic basis set. A range of energy level separations spanning the weak ($J \ll \omega$) and strong ($J \gg \omega$) electronic coupling regimes was explored. The vibronic coupling parameters are chosen to reflect typical values for molecular systems ranging from weak to moderate coupling. All parameters are scaled to the vibrational frequency ω_1 (which is set equal to 1.0), and represented as multiples of it. The magnitudes of the electronic dipole moments μ_1, μ_2, are set equal to 1.0, respectively, in arbitrary units, and the dipole directions assumed to be parallel.

For two excited electronic states, the above parameter description corresponds physically, e.g., to a molecular dimer with one excited state per molecule expressed in the electronic eigenstate (denoted by 1 and 2) representation. The coupling J is the splitting between these states while the condition $|\mu_1| = |\mu_2| = 1.0$ indicates that both eigenstates possess equivalent oscillator strength. The diagonal components of $\boldsymbol{\theta}_j$ represent the equilibrium shift of coordinate j from the ground state, while the off-diagonal component $\boldsymbol{\theta}_{12}$ induces mixing of the electronic eigenstates 1 and 2. For a symmetric dimer, the diagonal components can be interpreted as arising from symmetric coordinate motion, while the off-diagonal components arise from antisymmetric motion.

For strong electronic coupling (J large as compared to typical values of elements of $\boldsymbol{\theta}$), absorption into the one ($E < 0$) and two ($E > 0$) electronic manifolds are reasonably well separated, although the vibronic coupling produces both symmetric progressions and mixing. As J decreases, the two peaks merge into one; as $|\boldsymbol{\theta}|$ increases, the vibronic progressions become longer, and the spectrum tends toward that of a monomer (weak electronic coupling). Intermediate electronic coupling produces results between these extremes.

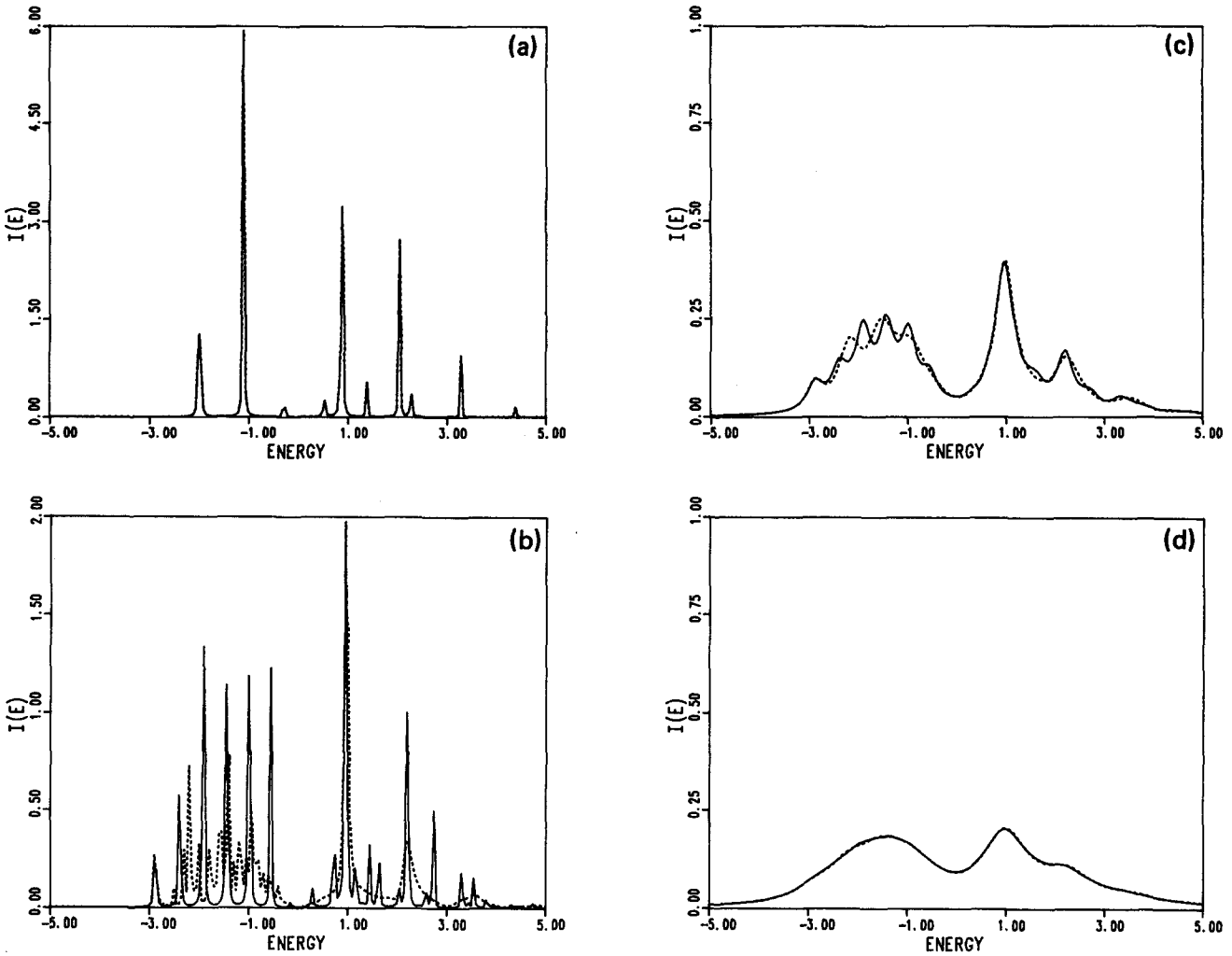

FIG. 1. Spectra at various resolutions. (a) Narrow band limit; (b) a typical vibronic coupling case at high resolution; (c) the same as (b) but at medium resolution; (d) the same as (b) but at low resolution.

The phenomenological damping factor γ is related to various line broadening factors and the lifetime of the excited states. The resolution of the optical spectrum is determined by γ. Three values of γ were investigated: (a) $\gamma = 0.01$ (high resolution) results in highly resolved spectra with many discrete lines, as are observed in gas phase experiments. (b) $\gamma = 0.2$ (medium resolution) yields a nontrivial vibronic peak structure, but without sharp individual lines. (c) $\gamma = 0.5$ (low resolution) produces a single broad peak (which may be significantly asymmetric). Spectra of types (b) and (c) can both be observed in condensed phase environments.

In the remainder of this section, we present graphs (Figs. 1–6) comparing the optical line shape $I(E)$ (in arbitrary units) from the basis set and matrix continued fraction calculations. The energy E is in units of the frequency ω_1 (which is set equal to 1.0). The dotted line is the result of Eq. (19), while the solid line is obtained from Eqs. (7)–(9). The numerical values of ω_j ($j \neq 1$) and the elements of ϵ and θ for Figs. 1–5 are given in Table I. The figure captions describe qualitatively the type of parameter set under study. For Fig. 6 (three-level system), parameter values are given in the figure captions.

When all modes have the same frequencies and vibronic coupling tensors (the single mode limit), the approximate Green's function reproduces exactly the spectra from the basis set calculation for any degree of resolution. A typical

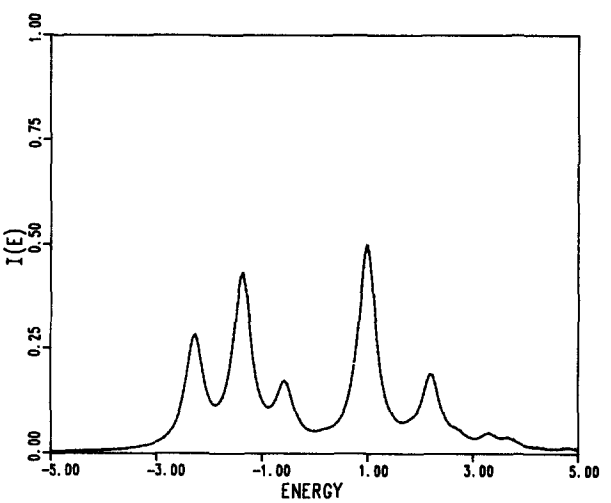

FIG. 2. A narrow band limit spectrum. The approximate Green's function method reproduces *high resolution* spectra from basis set calculations.

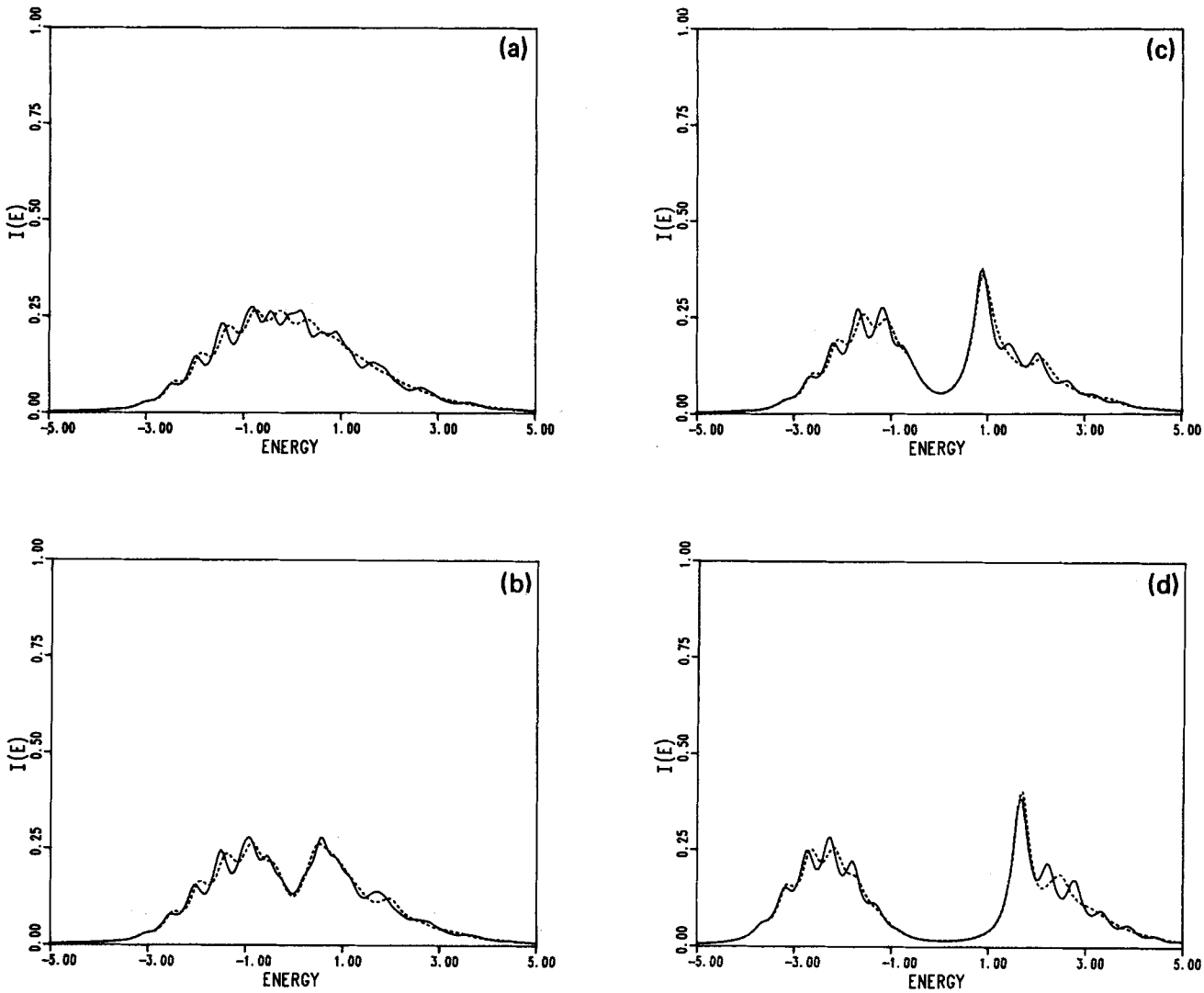

FIG. 3. Effects of different frequencies (i.e., $\omega_1 \neq \omega_2$). The value of ω_2 remains the same for the various electronic coupling values. (a) Weak electronic coupling; (b) intermediate electronic coupling; (c) intermediate electronic coupling; (d) strong electronic coupling.

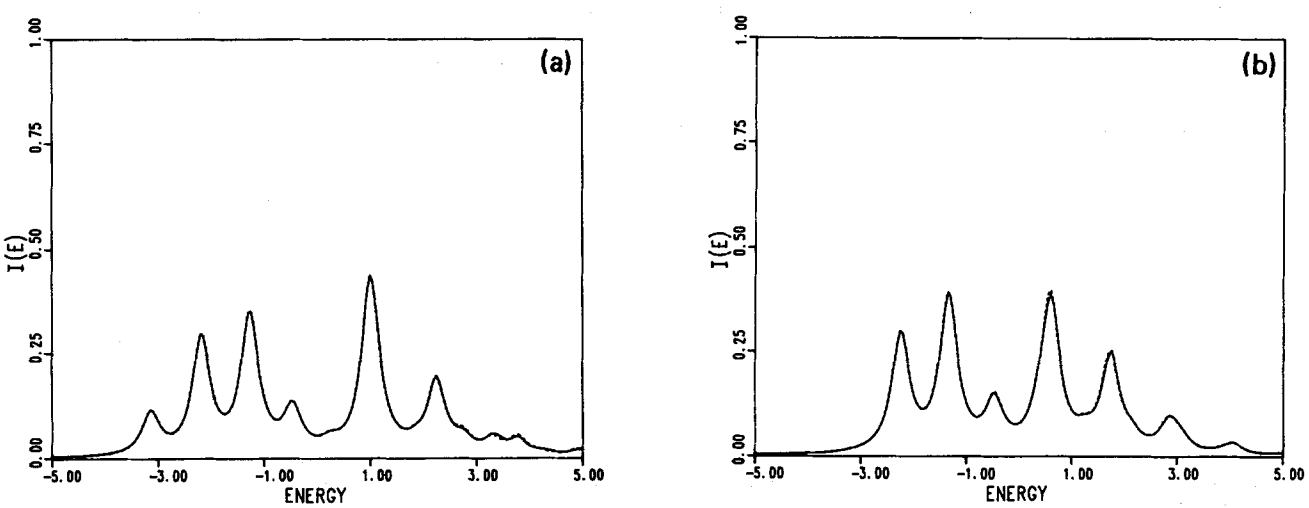

FIG. 4. Effects of different vibronic coupling tensors.

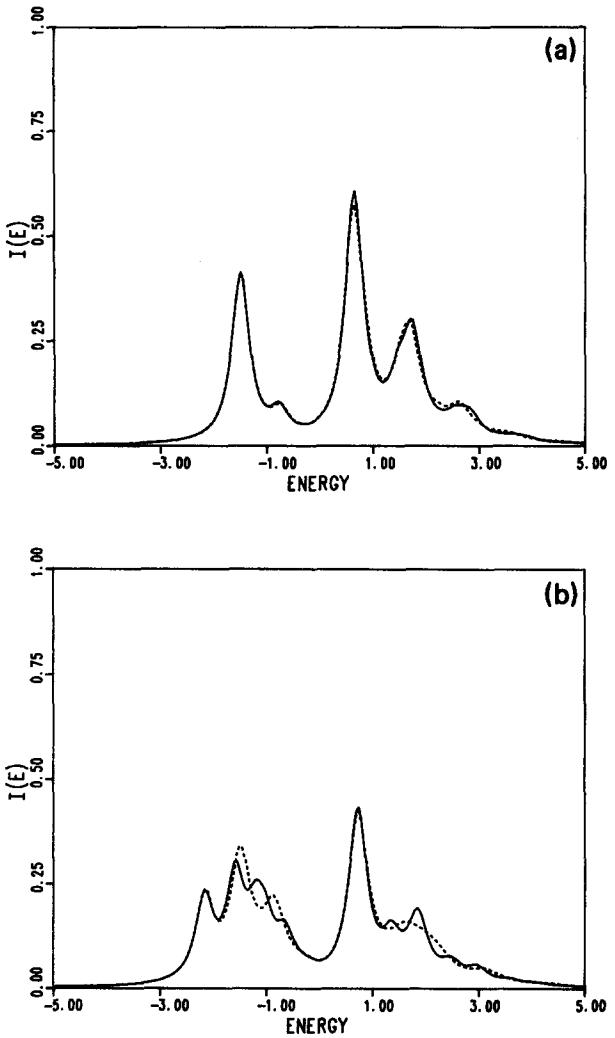

FIG. 5. Spectra for randomly chosen parameter sets.

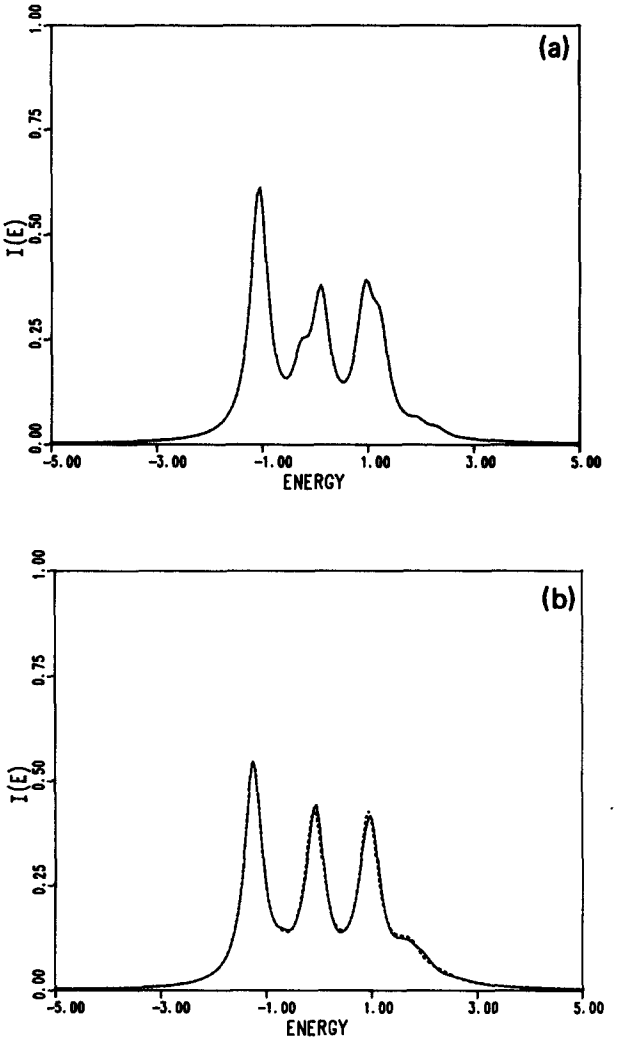

FIG. 6. Three-level three-mode system. Only the results for small vibronic coupling values are shown here. (a) A narrow band limit: $J = 1.0$, $\omega_1 = \omega_2 = \omega_3 = 1.0$, all $\theta_{ij} = 0.1$; (b) A different frequency case: $J = 2.0$, $\omega_2 = 0.8$, $\omega_3 = 0.6$, $\theta_{ii} = 0.2$, $\theta_{ij} = 0.1$ $(i \neq j)$.

TABLE I. Parameter values and basis set size for two-mode, two-level system numerical examples.[a]

Figure	J	ω^2	$g1d$	$g1n$	$g2d$	$g2n$	H matrix	γ
1(a)	1.0	1.0	0.5	0.4	0.5	0.4	450×450	0.01
1(b)	1.0	0.5	0.7	0.7	0.3	0.3	450×450	0.01
1(c)	1.0	0.5	0.7	0.7	0.3	0.3	450×450	0.20
1(d)	1.0	0.5	0.7	0.7	0.3	0.3	450×450	0.50
2	1.0	1.0	0.5	0.5	0.5	0.5	450×450	0.20
3(a)	0.1	0.5	0.5	0.5	0.5	0.5	450×450	0.20
3(b)	0.5	0.5	0.5	0.5	0.5	0.5	450×450	0.20
3(c)	1.0	0.5	0.5	0.5	0.5	0.5	450×450	0.20
3(d)	2.0	0.5	0.5	0.5	0.5	0.5	450×450	0.20
4(a)	1.0	1.0	0.5	0.5	0.7	0.7	450×450	0.20
4(b)	1.0	1.0	4b*	0.4	4b*	0.3	450×450	0.20
5(a)	5a*	0.8	0.5	0.3	0.4	0.2	162×162	0.20
5(b)	1.0	0.6	0.6	0.4	0.4	0.3	450×450	0.20

[a] All parameters are expressed in (energy) units of the vibrational frequency ω_1, which is set equal to 1.0. The column labeled "H matrix" gives the basis set size used in the numerical diagonalization procedure.
$\theta_{11}^{(1)} = \theta_{22}^{(1)} = g1d, \theta_{12}^{(1)} = \theta_{21}^{(1)} = g1n$; $\theta_{11}^{(2)} = \theta_{22}^{(2)} = g2d$, $\theta_{12}^{(2)} = \theta_{21}^{(2)} = g2n$.
4b* $\theta_{11}^{(1)} = 0.6$, $\theta_{22}^{(1)} = 0.7$; $\theta_{11}^{(2)} = 0.7$, $\theta_{22}^{(2)} = 0.5$.
5a* $\epsilon_{11} = 1.0$, $\epsilon_{12} = 0.5$, $\epsilon_{21} = 0.5$, $\epsilon_{22} = -1.0$.

high-resolution spectrum for a system in the single mode limit is shown in Fig. 1(a); all of the spectral lines are in excellent agreement with the basis set result.

As shown in Fig. 1(b), the approximation made on the continued fraction does not exactly reproduce highly resolved spectral lines ($\gamma = 0.01$) for systems with different frequencies and/or vibronic coupling tensors. However, the gross peak structures ($\gamma = 0.2$) and the spectral envelopes ($\gamma = 0.5$) are in good agreement [Figs. 1(c) and 1(d), respectively].

In the remainder of the paper we set γ equal to 0.2 (medium resolution), as the intended applications of our formalism are to condensed phase systems. Accurate simulation of gas-phase spectra requires use of an explicit basis set method.

We now consider the effects of variation in J, ω_2 and the elements of θ for a two-mode two-level excited state manifold.

Figure 2 illustrates that Eq. (19) is exact in the narrow band limit ($\omega_1 = \omega_2$, $\theta_1 = \theta_2$). This could also be proven analytically by means of a canonical transformation.

Figures 3(a)–3(d) shows the effect of setting ω_2 equal to 0.5. This results in some erroneous frequency denominators in the perturbation expansion of $\mathbf{G}(E)$ as compared to an exact prescription. As can be seen, at a resolution of $\gamma = 0.2$, the resulting error is quite small for all values of electronic coupling J, and despite use of moderate values (0.5) for the elements of θ. Calculations were also performed with all θ_{ij} set equal to 1.0. Agreement was generally acceptable, but the results are not shown here because the basis set results were not fully converged.

Differences in the vibronic coupling tensors θ_1 and θ_2 also lead to small discrepancies; here the numerators (coefficients) of exact diagrammatic expansion are only approximated by Eq. (19). As shown in Fig. 4, these effects are also small.

Figure 5 shows two typical spectra generated from a set of randomly chosen values of ω_2, θ_1, θ_2, and J. We have not uncovered a single two-mode two-level case where agreement at the $\gamma = 0.2$ resolution level is not comparable to that shown here (this does not rule out the possibility of disagreement for extremely large and different θ values, which we were unable to study because of failure of basis set convergence). Higher resolution agreement generally improves as $\omega_1 - \omega_2$, $\theta_1 - \theta_2$, and $|\theta_1|, |\theta_2|$ diminish (the last of these is due to exact limiting behavior in the second order of perturbation theory).

Figure 6 displays several calculations for an excited state manifold with three electronic states and three vibrational modes (192 basis functions were employed in the basis set method). Storage limitations restrict consideration to θ matrices of small amplitude; otherwise, it would be difficult to converge the basis set computations. For the examples presented, agreement of approximate and basis set methods is comparable to that for the two-level two-mode cases.

IV. CONCLUSIONS

At this point, it is appropriate to compare the approach in this paper with other work. Although the finite temperature and continuous phonon bandwidth versions of the theory will appear in a subsequent publication, our results to date indicate that they are equally successful; this will be assumed in what follows.

As stated in Ref. 1, the matrix continued fraction approach is a natural outgrowth of the work of Friesner and Silbey.[4] Greater accuracy is achieved at the cost of raising the computational effort from minimal to moderate, and obscuring the simplicity of the earlier work. Thus, the present method is preferable for quantitative studies. An additional benefit is the reliability of a single method for all electronic parameter regimes (weak and strong electronic coupling). This means that the partitioning scheme suggested in Ref. 1 (into high- and low-frequency vibrational modes) can be dispensed with in many cases.

As mentioned in the Introduction, perturbative approaches, whether in the electronic coupling constants (linear response theory,[7] classical coupled oscillator theory[6]) or in the exciton–phonon interaction,[2] have serious restrictions in their regions of validity. In addition, these methods ordinarily entail a Markovian approximation, which eliminates detailed spectral features. The variational small polaron method (the most flexible perturbative approach) shares this last defect, and is also invalid in the adiabatic limit.[5]

The degenerate ground state (DGS) theory of Hemenger[8] is also nonperturbative. However, it is difficult to generalize to finite temperature, computationally demanding for large clusters, and does not separate homogeneous and inhomogeneous broadening.[9] [For the present theory, inhomogeneous broadening is easily included by convoluting $\mathbf{G}(E)$ with appropriate functions.] Furthermore, accuracy with regard to complicated spectral envelopes has not yet been demonstrated.

The global accuracy of the present formalism at 0 K can be attributed to its exact treatment of electronic coupling and correct limiting behavior in both the narrow and wide phonon band (via the second order self-energy) regimes. The effect of additional approximations inherent in the finite temperature theory will be discussed elsewhere.

We note that inclusion of some high frequency vibronic levels in the $\mathbf{G}_0$ matrix (as suggested in Ref. 1) would lead to greater accuracy at high resolution. This approach will be explored in subsequent publications.

ACKNOWLEDGMENTS

This work was supported by grants from The Research Corporation and from The National Science Foundation. RAF is an Alfred P. Sloan Foundation fellow, 1984–86.

[1] R. Lagos and R. Friesner, J. Chem. Phys. **81**, 5899 (1984).
[2] B. West and K. Lindenberg (preprint).
[3] B. Jackson and R. Silbey, J. Chem. Phys. **75**, 3293 (1981).
[4] R. Friesner and R. Silbey, J. Chem. Phys. **76**, 1166 (1981); **75**, 925 (1891); **75**, 5630 (1981); R. Friesner, *ibid.* **76**, 2129 (1982).
[5] R. Friesner (unpublished results).
[6] H. Devoe, J. Chem. Phys. **41**, 393 (1964); **43**, 3199 (1965).
[7] W. Rhodes and M. Chase, Rev. Mod. Phys. **39**, 348 (1967).
[8] R. P. Hemenger, J. Chem. Phys. **66**, 1795 (1977); **68**, 1722 (1978); **67**, 262 (1977).
[9] R. Friesner, Chem. Phys. Lett. **84**, 361 (1985).
[10] R. E. Merrifield, Radiat. Res. **20**, 154 (1963).
[11] R. L. Fulton and M. Gouterman, J. Chem. Phys. **33**, 872 (1960).

[12]K. Cho and Y. Toyozawa, J. Phys. Soc. Jpn. **30**, 1555 (1971).
[13]N. S. Hush, in *Mixed Valence Compound*, edited by D. B. Brown (Reidel, Dordrecht, 1980).
[14]K. Y. Wong, P. N. Schatz, and S. E. Piepho, J. Am. Chem. Soc. **101**, 2793 (1979).
[15]A. Suna, Phys. Status Solidi B **45**, 591 (1971).
[16]H. Sumi, J. Phys. Soc. Jpn. **36**, 770 (1974); **38**, 825 (1975).
[17]I. B. Bersuker, *The Jahn–Teller Effect and Vibronic Interactions in Modern Chemistry* (Plenum, New York, 1984).
[18]J. Jortner, S. A. Rice, and R. M. Hochstrasser, Adv. Photochem. **7**, 149 (1969).
[19]J. Jortner and R. D. Levine, Adv. Chem. Phys. **47**, 1 (1981).
[20]J. Ulstrup, *Charge Transfer Processes in Condensed Media* (Springer, Berlin, 1979).
[21]R. Lagos and R. Friesner, Phys. Rev. B **29**, 3045 (1984).
[22]R. Lagos and R. Friesner, Chem. Phys. Lett. **122**, 98 (1985).